

Novel Measurements of Proton Structure at HERA

Katie Oliver
University of Oxford

On behalf of the H1 and ZEUS collaborations

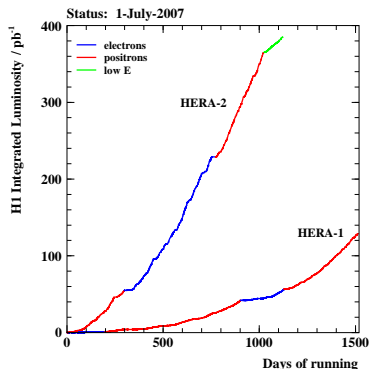
Rencontres de Moriond
QCD and High Energy Interactions
19th March 2010



HERA, H1 and ZEUS

HERA collided protons with longitudinally polarized e^\pm

- H1 and ZEUS were multi-purpose collider detectors at HERA
- 0.5 fb^{-1} luminosity taken by each experiment



HERA Energies

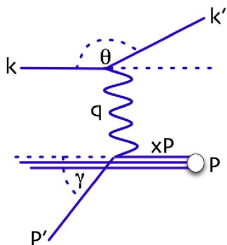
p beam: 920 GeV

e^\pm beam: 27.5 GeV

Centre of mass energy: 318 GeV

Mean polarization: 30 - 40%

Kinematics & Deep Inelastic Scattering



Neutral current
exchange of γ or Z^0
Charged current
exchange of W^\pm

Probing power of the lepton:

$$Q^2 = -q^2 = -(k - k')^2$$

$$= sxy$$

Bjorken scaling variable, the fraction of the proton's momentum carried by the struck quark

$$x = \frac{Q^2}{2p \cdot q}$$

Inelasticity, the energy fraction transferred from the lepton in the proton's rest frame

$$y = \frac{p \cdot q}{p \cdot k}$$

Centre of mass energy squared:

$$s = (p + k)^2$$

Neutral Current Cross Sections

Unpolarised neutral current reduced cross section

$$\tilde{\sigma}_{NC}^{e^\pm p} = \frac{xQ^4}{2\pi\alpha^2} \frac{1}{Y_+} \frac{d^2\sigma(e^\pm p)}{dx dQ^2} = F_2 \mp \frac{Y_-}{Y_+} xF_3 - \frac{y^2}{Y_+} F_L$$

- $Y_\pm \equiv 1 \pm (1 - y)^2$

Structure functions at Leading Order

F_2	$\propto \sum (q + \bar{q})$	Dominant contribution
xF_3	$\propto \sum (q - \bar{q})$	Contributes at high Q^2 (γZ interference)
F_L	$= 0$	Zero at Leading Order

Charged Current Cross Sections

Charged current reduced cross section

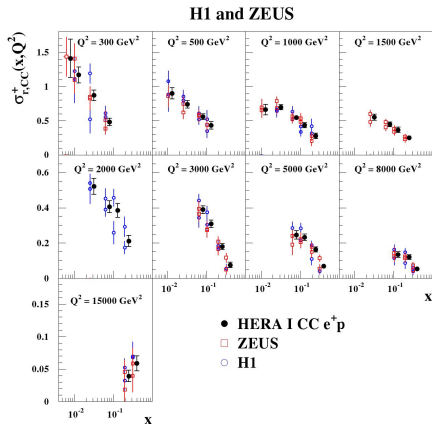
$$\tilde{\sigma}(e^-p)_{CC} = (1 - P_e) [u + c + (1 - y)^2(\bar{d} + \bar{s})]$$

$$\tilde{\sigma}(e^+p)_{CC} = (1 + P_e) [\bar{u} + \bar{c} + (1 - y)^2(d + s)]$$

- Linear polarisation dependence
- Electron (positron) data is sensitive to u (d) valence quark
- Probes flavour structure of the proton

HERA-I Inclusive Cross Section Combination

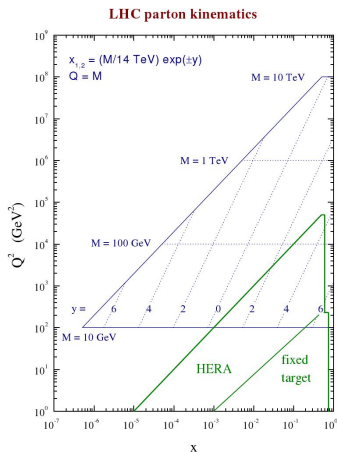
- H1 & ZEUS have combined inclusive cross sections from HERA I data ($\sim 115 \text{ pb}^{-1}$ per experiment)
- Combination procedure:
 - 1 Swim all points to a common $Q^2 - x$ grid
 - 2 Move 820 GeV data to 920 GeV p-beam energy
 - 3 Calculate average values and uncertainties
 - 4 Evaluate procedural uncertainties
- Data combination uses χ^2 minimisation method



Overall precision is improved
 $\chi^2/\text{NDF} = 637/656$

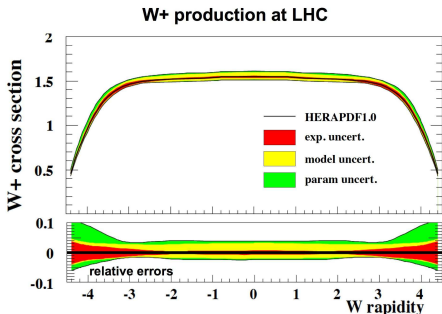
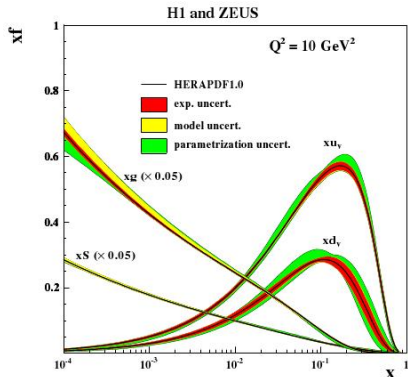
QCD Fits

- NC and CC reduced cross sections are the main input used to determine Parton Distribution Functions (PDFs) by performing QCD Fits
- Measure $\tilde{\sigma}$ for polarised data
- Obtain F_2 , xF_3 and extract the PDFs: $q(x, Q^2)$, $\bar{q}(x, Q^2)$, $g(x, Q^2)$
- Proton PDFs are an important input for LHC physics
- Evolve PDFs to the LHC kinematic region with DGLAP equations
- Only need to evolve in Q^2 since HERA x range is comparable to that of LHC



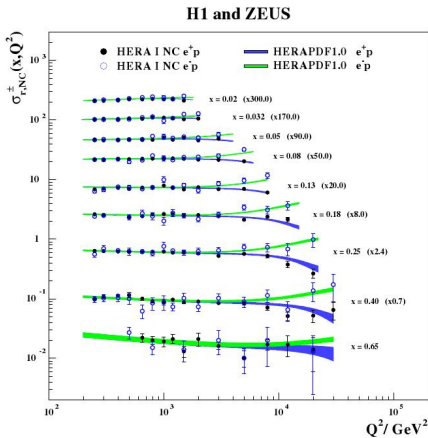
HERAPDF1.0

Combined HERA-I data are the sole input in determination of a new set of PDFs with small experimental uncertainties: HERAPDF1.0



Combined Data With HERAPDF1.0

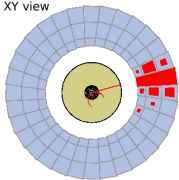
- HERA-I data:
 - Good sensitivity at low Q^2
 - BUT limited statistical precision at high Q^2
- HERA-II data not yet included:
further improvement possible!



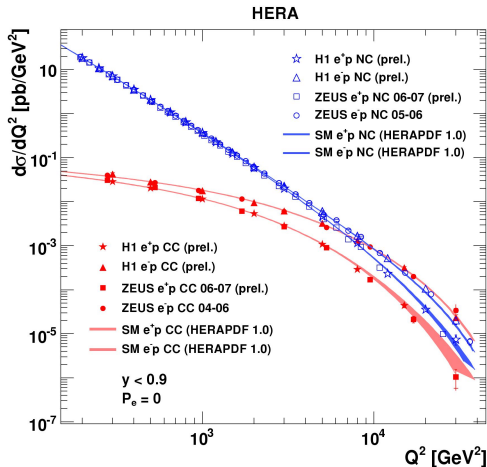
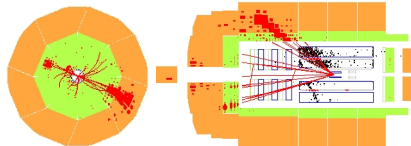
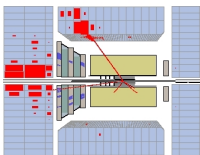
JHEP01 (2010) 109

Charged Current & Neutral Current at HERA-II

XY view



ZR view

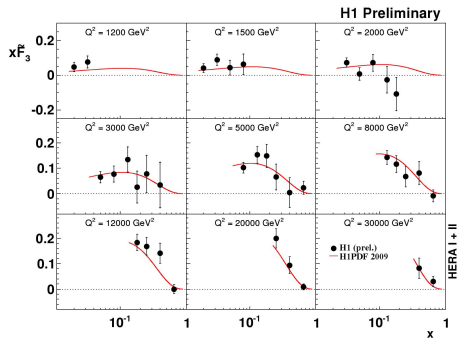
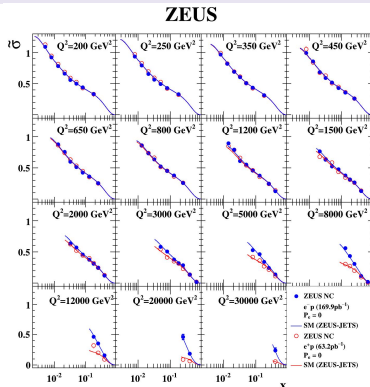


Higher statistics \Rightarrow improved precision

High Q^2 NC Cross Sections I

Eur. Phys. J. C 62 (2009) 625-658

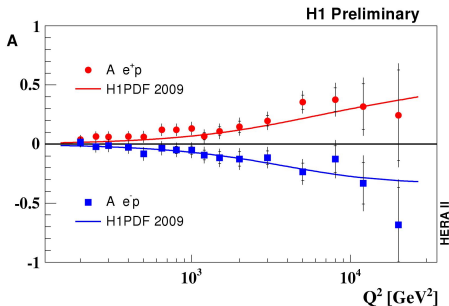
H1prelim-09-042



$$\tilde{\sigma}_{NC}^{e^\pm p} \approx F_2 \mp \frac{Y_-}{Y_+} xF_3 \quad \text{and} \quad x\tilde{F}_3 = \frac{Y_+}{2Y_-} \left(\tilde{\sigma}^{e^-p} - \tilde{\sigma}^{e^+p} \right) \approx \frac{x}{3} (2u_v + d_v)$$

High Q^2 NC Cross Sections II

Polarization asymmetry provides a direct measure of EW effects:
NC parity violation observed at EW scale

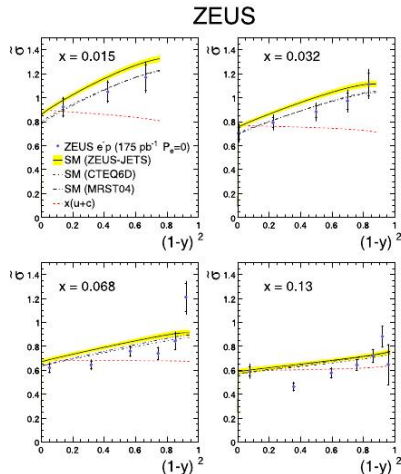
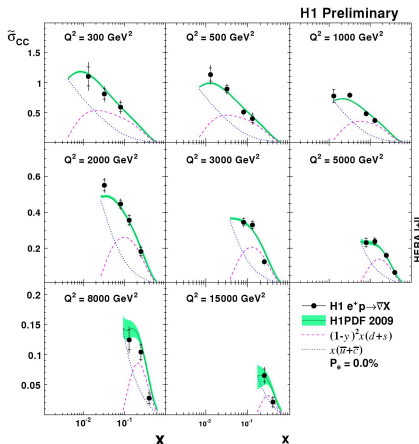


$$A^{\pm} = \frac{2}{P_e^+ - P_e^-} \left(\frac{\sigma^{\pm}(P_e^+) - \sigma^{\pm}(P_e^-)}{\sigma^{\pm}(P_e^+) + \sigma^{\pm}(P_e^-)} \right)$$

High Q^2 CC Cross Sections I

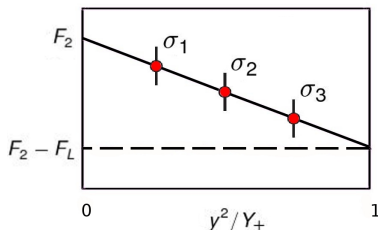
H1prelim-09-043

Eur. Phys. J. C 61 (2009) 223-235



F_L I

- At NLO, $F_L \propto \alpha_s xg(x, Q^2)$. F_L contributes at high y , low Q^2
- F_L has not previously been measured directly: gluon density was derived from scaling violations in F_2
- Direct F_L measurement requires measurement of the reduced cross sections at same x and Q^2 but different y
- $Q^2 = sxy \Rightarrow$ different $y \leftrightarrow$ different $s \leftrightarrow$ different beam energies



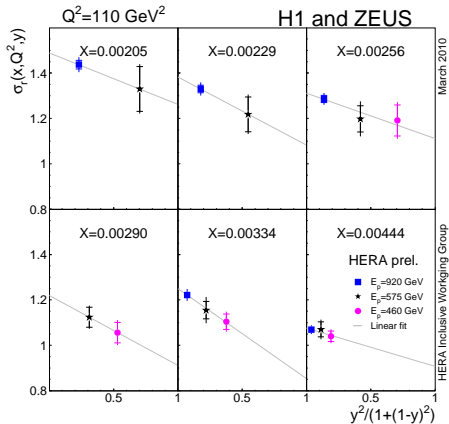
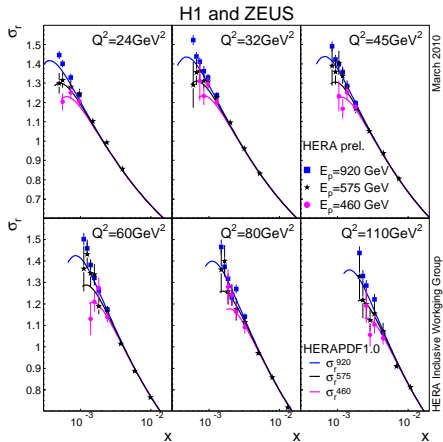
Low Q^2 NC reduced cross section

$$\tilde{\sigma}_{NC}^{e^{\pm}p} = F_2(x, Q^2) - \frac{y^2}{Y_+} F_L(x, Q^2)$$

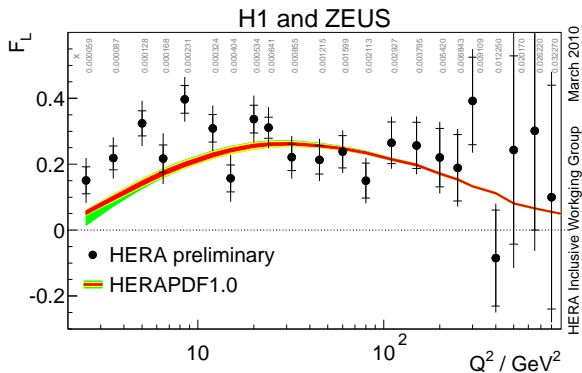
At given x and Q^2 : F_2 is the intercept at y -axis, F_L is the negative slope

F_L II

NEW: ZEUS and H1 combination



E_p (GeV)	\sqrt{s} (GeV)	\mathcal{L} (pb^{-1})
920	318	21.6
575	251	6.2
460	225	12.4

F_L III

- F_L is extracted in region: $2.5 < Q^2 < 800 \text{ GeV}^2$
- A new and important input to QCD

Published:

H1: Phys. Lett. B665 (2008) 139-146

ZEUS: Phys. Lett. B682 (2009) 8-22

Combined:

H1prelim-10-043

ZEUS-prel-10-001

Summary

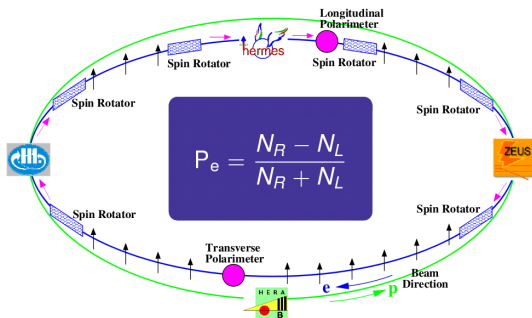
- A lasting legacy of HERA is a far greater understanding of the structure of the proton
- H1 and ZEUS will continue to combine data to achieve greater precision
- HERA data is necessary for precise predictions at the LHC



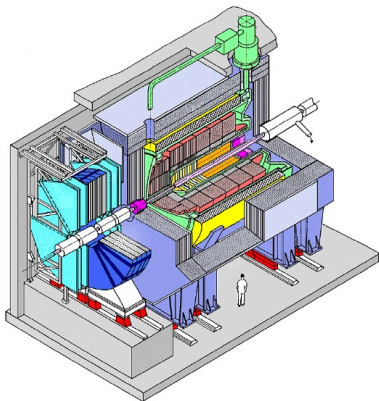
Back-Up Slides

HERA: Polarised Lepton Beam

- e beam becomes transversely polarized through emission of synchrotron radiation
- Spin rotators were installed during the HERA upgrade to obtain longitudinal polarization at both IPs
- Mean (lumi weighted) polarization achieved: 30 - 40%



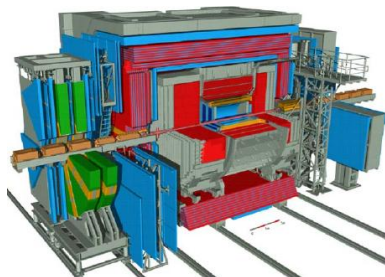
H1



- Hermetic - 4π detector
- Tracking:
 - Central drift chamber
 - Silicon Microvertex detector
- Liquid-argon calorimeter (LAr)
- Rear lead-scintillator (SPACAL)
- μ chambers

Optimised for precision measurement of the scattered electron

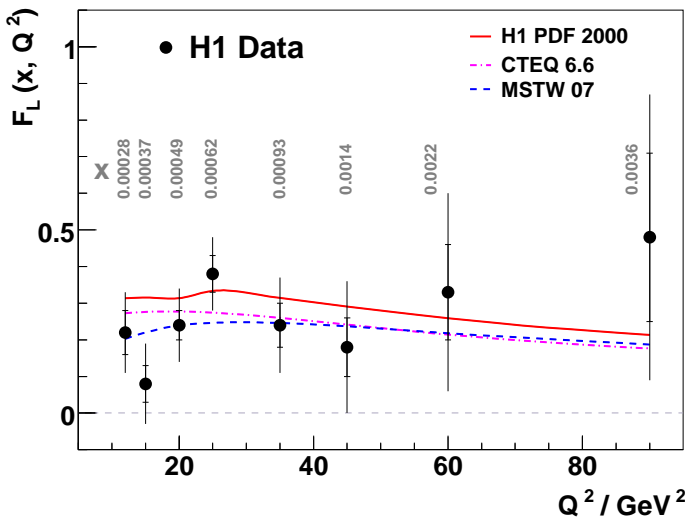
ZEUS



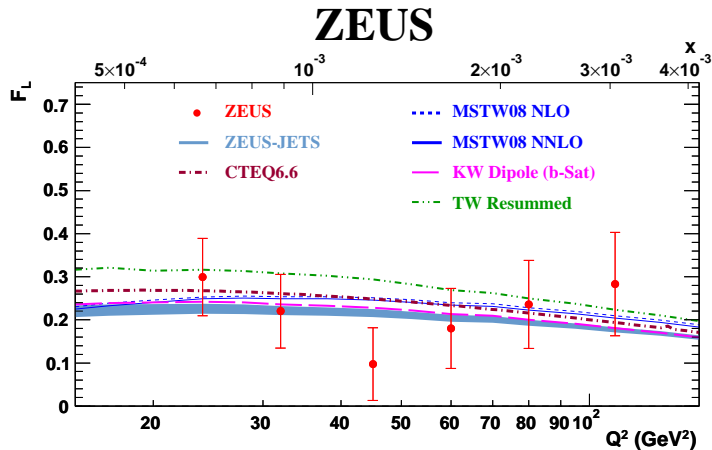
- Hermetic - 4π detector
- Tracking:
 - Central Tracking Detector (CTD), a cylindrical drift chamber
 - Silicon Microvertex detector (MVD) (HERA-II)
- Compensating uranium scintillator calorimeter (UCAL)
- μ chambers

Optimised for precision measurement of the hadronic final state

F_L : H1 Comparison To Theory Curves



F_L : ZEUS Comparison To Theory Curves



F_L : Indirect Measurement

Low Q^2 reduced cross section $\tilde{\sigma}^{NC}$

$$\tilde{\sigma}^{NC} = F_2(Q^2, x) - \frac{y^2}{Y_+} F_L(x, Q^2)$$

- Derivative method:

$$\left. \frac{d\tilde{\sigma}}{d \ln y} \right|_{Q^2} \approx \left. \frac{dF_2}{d \ln y} \right|_{Q^2} - \frac{2y^2(2-y)}{Y_+^2} F_L$$

- Derivative dominated by F_L term at high y
- Shape method:

$$\tilde{\sigma}_{fit} = cx^{-\lambda} - \frac{y^2}{Y_+} F_L$$

- Shape driven by kinematic factor rather than F_L

F_2 & F_3

Consider the total cross-section: $\sigma^0 + P\sigma^P$:

The unpolarised cross-section is given by $\sigma^0 = Y_+ F_2^0 + Y_- xF_3^0$:

- $F_2^0 = \sum_i A_i^0(Q^2)[xq_i(x, Q^2) + x\bar{q}_i(x, Q^2)]$
- $xF_3^0 = \sum_i B_i^0(Q^2)[xq_i(x, Q^2) - x\bar{q}_i(x, Q^2)]$
- $A_i^0(Q^2) = e_i^2 - 2e_i v_i v_e P_Z + (v_e^2 + a_e^2)(v_i^2 + a_i^2)P_Z^2$
- $B_i^0(Q^2) = -2e_i a_i a_e P_Z + 4a_i a_e v_i v_e P_Z^2$

The polarised cross-section is given by $\sigma^P = Y_+ F_2^P + Y_- xF_3^P$:

- $F_2^P = \sum_i A_i^P(Q^2)[xq_i(x, Q^2) + x\bar{q}_i(x, Q^2)]$
- $xF_3^P = \sum_i B_i^P(Q^2)[xq_i(x, Q^2) - x\bar{q}_i(x, Q^2)]$
- $A_i^P(Q^2) = 2e_i v_i a_e P_Z - 2v_e a_e (v_i^2 + a_i^2)P_Z^2$
- $B_i^P(Q^2) = 2e_i a_i v_e P_Z - 2a_i v_i (v_e^2 + a_e^2)P_Z^2$

$$P_Z = \frac{Q^2}{(M_Z^2 + Q^2) \sin^2(2\theta_W)}$$

$P_Z \gg P_Z^2$ (γZ interference dominant)

v_e very small (~ 0.04)

so:

Unpolarised $xF_3 \rightarrow a_i$

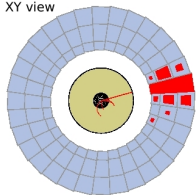
Polarised $F_2 \rightarrow v_i$

Charged Current & Neutral Current Events

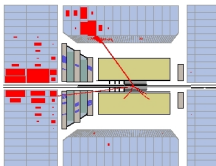
CC Event: Large missing transverse momentum (p_T) due to neutrino

NC Event: High p_T isolated scattered electron/positron and balanced total p_T

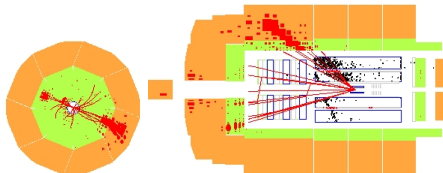
XY view



ZR view



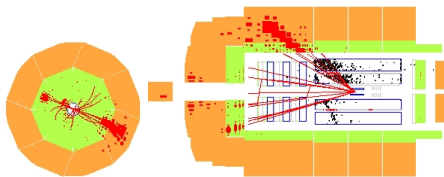
Final selection: $\sim 10^3$ events per sample



Final selection: $\sim 10^5$ events per sample

Neutral Current Event Selection

High p_T isolated scattered electron/positron and balanced total p_T



- Suppress photoproduction background: conserve longitudinal energy-momentum:
 $\delta = E - p_z \approx 2E_e$
- Final selection: $\sim 10^5$ events per sample

Kinematic reconstruction: angle and energy of scattered electron

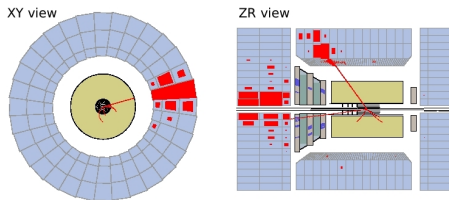
$$Q_{el}^2 = 2E_e E'_e (1 + \cos \theta_e)$$

$$y_{el} = 1 - \frac{E'_e}{2E_e} (1 - \cos \theta_e)$$

$$x_{el} = \frac{E_e}{E_p} \frac{E'_e (1 + \cos \theta_e)}{2E_e - E'_e (1 - \cos \theta_e)}$$

Charged Current Event Selection

Large missing transverse momentum (p_T) due to neutrino



- Suppress dominant background (photoproduction)
- Topological finders to remove cosmic muons
- Final selection: $\sim 10^3$ events per sample

Kinematic reconstruction from hadrons (Jacquet-Blondel)

$$\delta = \sum_i (E^i - p_z^i)$$

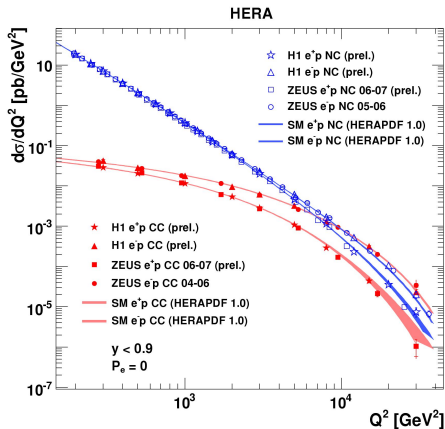
$$p_T^2 = (\sum_i p_x^i)^2 + (\sum_i p_y^i)^2$$

$$Y_{JB} = \frac{\delta}{2E_e}$$

$$X_{JB} = \frac{p_T^2}{sY_{JB}(1-Y_{JB})}$$

$$Q_{JB}^2 = sX_{JB}Y_{JB}$$

High Q^2 NC and CC Cross Sections

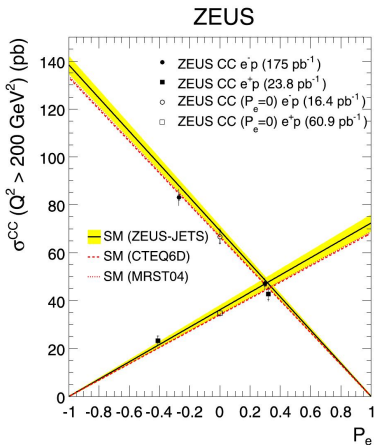


- NC and CC high Q^2 cross sections are measured very precisely over many orders of magnitude in Q^2

High Q^2 CC Cross Sections II

$$\sigma_{CC}^{e^\pm p}(P_e) = (1 \pm P_e)\sigma_{CC}^{e^\pm p}(P_e = 0)$$

- Tests chiral nature of the SM
- Do not constrain linear fit to zero at $P_e = +1$ ($P_e = -1$) for electrons (positrons)
- Assume non-zero cross section due to a right-handed W boson (W_R)
- Derive lower limit on mass of W_R assuming:
 - $g_L = g_R$
 - Light ν_R



	Electron	Positron
H1	186 GeV	208 GeV
ZEUS	180 GeV	

ZEUS & H1 Combination Method

Data Set		x Range		Q^2 Range GeV ²		\mathcal{L} pb ⁻¹	e^+/e^-
H1 svx-mb	95-00	5×10^{-6}	0.02	0.2	12	2.1	$e^+ p$
H1 low Q^2	96-00	2×10^{-4}	0.1	12	150	22	$e^+ p$
H1 NC	94-97	0.0032	0.65	150	30000	35.6	$e^+ p$
H1 CC	94-97	0.013	0.40	300	15000	35.6	$e^+ p$
H1 NC	98-99	0.0032	0.65	150	30000	16.4	$e^- p$
H1 CC	98-99	0.013	0.40	300	15000	16.4	$e^- p$
H1 NC HY	98-99	0.0013	0.01	100	800	16.4	$e^- p$
H1 NC	99-00	0.0013	0.65	100	30000	65.2	$e^+ p$
H1 CC	99-00	0.013	0.40	300	15000	65.2	$e^+ p$
ZEUS BPC	95	2×10^{-6}	6×10^{-5}	0.11	0.65	1.65	$e^+ p$
ZEUS BPT	97	6×10^{-7}	0.001	0.045	0.65	3.9	$e^+ p$
ZEUS SVX	95	1.2×10^{-5}	0.0019	0.6	17	0.2	$e^+ p$
ZEUS NC	96-97	6×10^{-5}	0.65	2.7	30000	30.0	$e^+ p$
ZEUS CC	94-97	0.015	0.42	280	17000	47.7	$e^+ p$
ZEUS NC	98-99	0.005	0.65	200	30000	15.9	$e^- p$
ZEUS CC	98-99	0.015	0.42	280	30000	16.4	$e^- p$
ZEUS NC	99-00	0.005	0.65	200	30000	63.2	$e^+ p$
ZEUS CC	99-00	0.008	0.42	280	17000	60.9	$e^+ p$

Combination Method: χ^2

$$\chi_{\text{exp}}^2(\mathbf{m}, \mathbf{b}) = \sum_i \frac{[m^i - \sum_j \gamma_j^i m^i b_j - \mu^i]^2}{\delta_{i,\text{stat}}^2 \mu^i (m^i - \sum_j \gamma_j^i m^i b_j) + (\delta_{i,\text{uncor}} m^i)^2} + \sum_j b_j^2.$$

$$\chi_{\text{tot}}^2(\mathbf{m}, \mathbf{b}') = \chi_{\text{min}}^2 + \sum_{i=1}^{N_M} \frac{[m^i - \sum_j \gamma_j^{i,\text{ave}} m^i b'_j - \mu^{i,\text{ave}}]^2}{\delta_{i,\text{ave,stat}}^2 \mu^{i,\text{ave}} (m^i - \sum_j \gamma_j^{i,\text{ave}} m^i b'_j) + (\delta_{i,\text{ave,uncor}} m^i)^2} + \sum_j (b'_j)^2.$$

μ^i	Measured value at point i
γ_j^i	Relative correlated systematic
$\delta_{i,\text{stat}}$	Relative statistical uncertainty
$\delta_{i,\text{uncor}}$	Relative uncorrelated systematic uncertainty
m^i	Prediction for measurement
b_j	Shifts of correlated error sources

Combination Method: Procedural Uncertainties

- Additive vs multiplicative nature of the error sources
 - typically below 0.5%
- A study of the possible correlated systematic uncertainties between H1 and ZEUS was performed:
 - Identified 12 possible uncertainties of common origin
 - Compared 212 averages taking all pairs as correlated/uncorrelated in turn
 - Mostly negligible except for:
 - 1 Correlated systematic uncertainty for the photoproduction background (few % at high- y)
 - 2 Correlated systematic uncertainty for the hadronic energy scale (at the per mille level)

Combination Method: Uncertainties

- 1402 points are combined to 741 unique cross section measurements
- $\chi^2/NDF = 637/656$
- 110 systematic errors from the experimental considerations
- 3 procedural systematic errors
- Overall precision:
 - $3 < Q^2 < 500$ GeV: 2% precision
 - $20 < Q^2 < 100$ GeV: 1% precision

Combination Method: Cross-Calibration

- Several correlated systematic uncertainties are reduced considerably for the averaged result:
 - Uncertainty on H1 calorimeter energy scale reduced by 55%
 - Uncertainty on ZEUS γP background reduced by 65%
- Different reconstruction methods \Rightarrow similar systematic sources influence cross sections differently as a function of Q^2 and x
 - Requiring agreement at all Q^2 and x constrains systematics
- In some regions, one experiment has better precision
 - The less precise measurement is fitted to the more precise one
 - Reduction in correlated systematic uncertainty

PDF Details

Scheme:	Thorne-Roberts VFNS
Evolution:	QCDNUM
Order:	NLO
Q_0^2	1.9 GeV ²
f_s	0.31
Renormalisation scale:	Q^2
Factorisation scale:	Q^2
Q_{min}^2	3.5 GeV ²
$\alpha_S(M_W)$	0.1176
M_c	1.4 GeV
M_b	4.75 GeV

PDF Experimental Uncertainties

- Uncorrelated uncertainties:
 - Statistical errors
 - Point-to-point uncorrelated uncertainties:
 - e.g statistical errors due to MC simulations
 - Are added in quadrature to the statistical errors
- Correlated uncertainties:
 - Point-to-point correlated uncertainties:
 - e.g. electromagnetic and hadronic energy scale calibration
 - often common for CC and NC for a given experiment and run period
- Overall normalisation uncertainty:
 - Correlated for all data points for a given experiment and run period
- Correlations between H1 and ZEUS:
 - H1 and ZEUS use similar analyses methods
 - Largest from γP background and hadronic energy scales

PDF Model Uncertainties

Variation	Standard Value	Lower Limit	Upper Limit
f_s	0.31	0.23	0.38
m_c [GeV]	1.4	1.35 ^(a)	1.65
m_b [GeV]	4.75	4.3	5.0
Q_{min}^2 [GeV ²]	3.5	2.5	5.0
Q_0^2 [GeV ²]	1.9	1.5 ^(b)	2.5 ^(c,d)

$$^{(a)}Q_0^2 = 1.8$$

$$^{(c)}m_c = 1.6$$

$$^{(b)}f_s = 0.29$$

$$^{(d)}f_s = 0.34$$

- Numerical values used for the central fit are varied
- Difference between the nominal fit and fits corresponding to model variations are added in quadrature
 \Rightarrow Total model uncertainty

PDF Parametrisation Uncertainties

- 1 Variation in Q_0^2 (starting scale)
- 2 Negative gluon contribution at low- x is allowed
- 3 $B_{u_v} \neq B_{d_v}$ for u_v and d_v parametrisations:

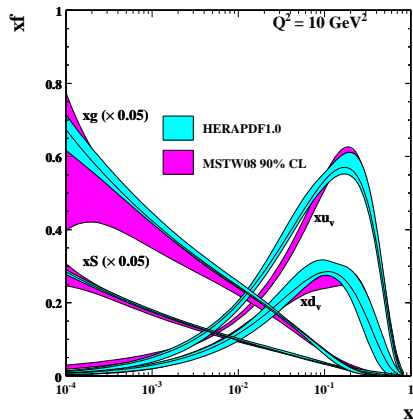
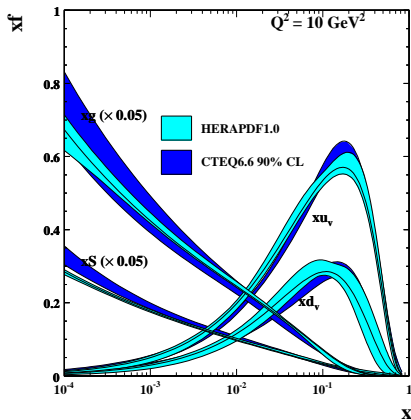
$$\begin{aligned}x u_v(x) &= A_{u_v} x^{B_{u_v}} (1-x)^{C_{u_v}} (1 + E_{u_v} x^2) \\x d_v(x) &= A_{d_v} x^{B_{d_v}} (1-x)^{C_{d_v}}\end{aligned}$$

- 4 Variation in number of terms in the polynomial:

$$xf(x) = Ax^B(i-x)^C(1 + \epsilon\sqrt{(x)} + Dx + Ex^2)$$

Envelope representing the maximum deviation at each x value is constructed to represent the parametrisation uncertainty

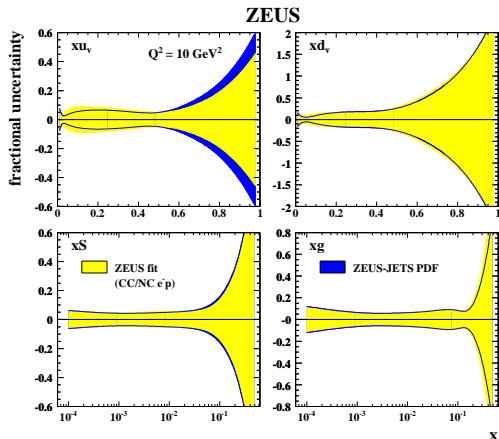
HERAPDF1.0: Comparison to Other PDFs



ZEUSfit09: Adding High Q^2 NC and CC Polarised e^-p Data

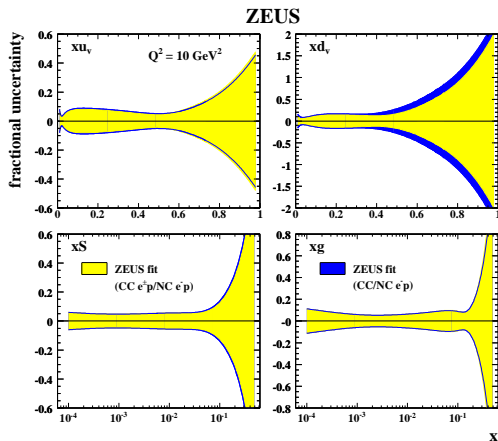
The ZEUS-JETS PDF was modified by incorporating:

- 1 high- Q^2 NC polarised e^-p data: Eur. Phys. Journal C 62 (2009) 625-658)
- 2 high- Q^2 CC polarised e^-p data: Eur. Phys. Journal C 61 (2009) 223-235)



ZEUSfit09: Adding High Q^2 CC Polarised e^+p Data

In addition, high- Q^2 CC polarised e^+p data was added (ZEUS-prel-09-002)



ZEUSfit09: Adding High Q^2 NC and CC Polarised e^-p and High Q^2 CC Polarised e^+p Data

The ZEUS-JETS PDF was modified by incorporating:

- 1 high- Q^2 NC polarised e^-p data: Eur. Phys. Journal C 62 (2009) 625-658
- 2 high- Q^2 CC polarised e^-p data: Eur. Phys. Journal C 61 (2009) 223-235
- 3 high- Q^2 CC polarised e^+p data: ZEUS-prel-09-002

